

## **EFFECTS OF MECHANICALLY DRILLED PITS ON TENSILE DUCTILITY AND FRACTURE BEHAVIOR OF A STRUCTURAL STEEL**

**Somayeh ALIPOUR, Hassan FARHANGI and Changiz DEGHANIAN**

School of Metallurgy and Materials Engineering, Faculty of Engineering,  
University of Tehran, Tehran, Iran.

### **ABSTRACT**

Geometrical discontinuities resulting from localized pitting can lead to substantial degradation of mechanical properties of steel structures especially in marine environments. This effect is usually evaluated in terms of the reduced section thickness associated with pit geometry which lowers the load carrying capacity of the structure. In this research, the effects of depth, spacing, and distribution of artificially produced, pit like, discontinuities on tensile ductility and fracture behavior of a structural steel have been investigated. Simulated pit distributions were produced on the gage sections of flat tensile specimens using mechanical drilling. A series of tensile tests were performed on specimens with pit area percents from 4 to 64% and various pith depths and spacing. It was found that fracture strain was substantially reduced at low pit area percents, but tended to partially recover at high pit area percents. This effect was further intensified by increasing pith depth. Furthermore, a change in the fracture surface orientation and formation of multiple secondary cracks were noted in pit distributions with higher stress concentration factors. SEM fractographs are presented to characterize the fracture surface morphologies. The overall findings are discussed in terms of mutual interaction of multiple stress concentration sites, triaxial stress state, and strain localization.

**Keywords:** Final elongation, Fractography, Pit area percent, Pit spacing, Tensile strength.

### **1. INTRODUCTION**

Existence of geometrical discontinuities like holes or notches in materials causes non-uniform stress distributions around the discontinuities. So each geometrical discontinuity acts as a stress concentration site [1,2]. Pitting corrosion represents an important limitation to the safe and reliable use of many alloys in various industries. Pitting is a very serious type of corrosion damage because of the rapidity with which metallic sections might be perforated. The unanticipated occurrence of pitting and its unpredictable propagation rate make it difficult to take it into consideration in practical engineering designs [3]. Pitting corrosion can adversely affect the load carrying capacity of structures due to the stress concentration effect and reduced section thickness associated with pit geometry. For localized corrosion such as pitting, the strength calculation procedure can be more complex [4]. Size, shape and depth of pits can be effective factors on strength but from this point of view no more researches have been done, so far. Recently, Tatsuro Nakai et al. [5,6] evaluated pitting corrosion effects on structural strength of hold frames of cargo holds of bulk carriers which exclusively carry coal and iron ore. The moisture of coal and iron ore cause pitting corrosion of bulk carrier [7].

Their evaluation was carried out by using artificial pits on the specimen's surfaces by drilling to simulate pitting corrosion. They showed that the trend of actual corroded specimens corresponds well with that of the artificially pitted specimens. So it is possible to predict the mechanical properties of pitted sections by virtue of this result [5,8]. In the present research artificial pits are also used to simulate pitting corrosion. However, the effects of additional factors not previously considered, such as spacing and area percent of pits, on tensile strength and percent final elongation of ST52 steel plates is also investigated. The main scope of the activity of the failure analysis performed in this investigation was to identify the failure mechanism of the insert bolts and to clarify the role of material deficiencies with respect to the operative failure mechanism.

## 2. EXPERIMENTAL METHODS

ST52 steel plates were used in this study as a structural material to simulate the effects of corrosion pits on mechanical properties. The chemical composition of ST52 steel used in the investigation is given in Table 1. Specimens were cut out parallel to the rolling direction of the plate with 5 mm thickness.

**Table 1.** Chemical composition of ST52 steel.

| Alloy type | Composition (wt. %) |      |      |       |       |      |       |       |      |         |
|------------|---------------------|------|------|-------|-------|------|-------|-------|------|---------|
|            | C                   | Si   | Mn   | P     | S     | Cr   | V     | Nb    | Cu   | Fe      |
| ST52 steel | 0.135               | 0.01 | 0.86 | 0.014 | 0.011 | 0.02 | 0.058 | 0.021 | 0.02 | balance |

Flat tensile specimens for tensile testing were machined according to the E8M ASTM standard. The specimen dimensions including width (W), gauge length (G) and total length (L) of specimens were 40, 50 and 200 mm, respectively, as shown in Figure 1.

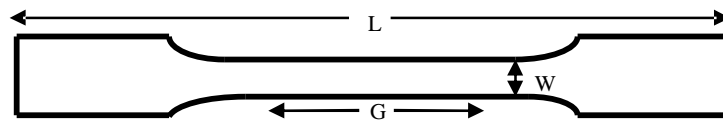


**Figure 1.** Tensile test specimen.

The artificial pits were made on a surface between the gauge marks by drilling to simulate pitting corrosion. The shape of the artificial pits was determined based on the actually observed and reported geometry of corrosion pits on hold frames of bulk carriers [5]. The shape adopted in this experiment is a circular cone and the pit diameter employed is 4 mm. Cross-sectional view of the corrosion pits is shown in Figure 2.

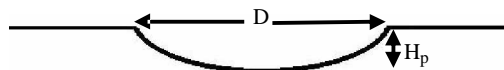


**Figure 2.** The cross-sectional view of an artificial pit.

Fourteen kinds of pit distribution (Fig. 3) are employed to investigate the effect of pits area percent and pit distribution on fracture behavior. These are tabulated in Table 2 together with number of pits, pit spacing and pit area percent.

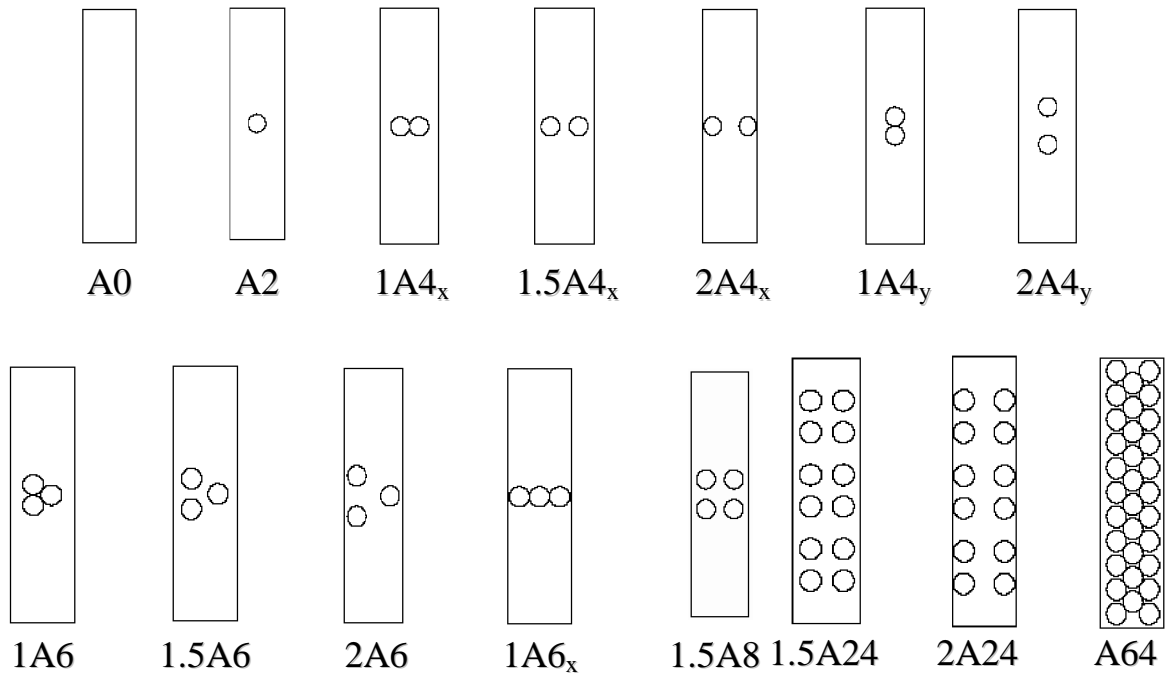


**Figure 3.** Schematic of several kinds of pit distributions

**Table 2.** Types of pit distributions.

| No.              | Number of pits | Pit area percent | Pit spacing |
|------------------|----------------|------------------|-------------|
| A0               | 0              | 0                | -           |
| A2               | 1              | 2                | -           |
| 1A4              | 1              | 4                | 1D          |
| 1.5A4            | 2              | 4                | 1.5D        |
| 2A4              | 2              | 4                | 2D          |
| 1A6              | 3              | 6                | 1D          |
| 2A6              | 3              | 6                | 2D          |
| 1A6 <sub>x</sub> | 3              | 6                | 1D          |
| 1.5A8            | 4              | 8                | 1.5D        |
| 1.5A10           | 5              | 10               | 1.5D        |
| 1.5A24           | 12             | 24               | 1.5D        |
| 2A24             | 12             | 24               | 2D          |
| A64              | 32             | 64               | 1D          |

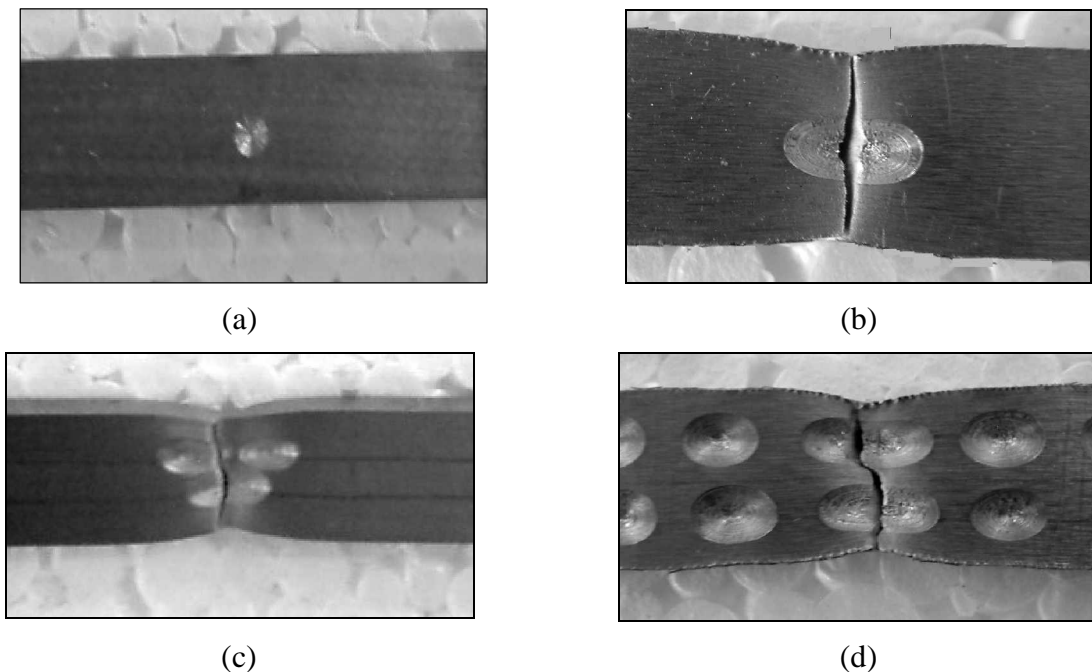
Pit area percent (PAP) is defined as percentage of the surface area covered with pits between the gauge marks. Pit diameter (D) of these specimens is 4 mm. For the purpose of investigating the effect of pit spacing ( $L_p$ ), nineteen specimens were prepared. The pit spacing

defined as a multiple of pit diameter ( $D$ ) based on the center to center distance between the pits, ranged from  $1D$  to  $2D$ . Also several pit distribution with pit depths ( $H_p$ ) of 0.5, 1, and 1.5 mm were considered. All tensile tests were carried out at a nominal strain rate of  $5 \times 10^{-4} \text{ s}^{-1}$ . The fractured tensile specimens were first subjected to visual examination and macrofractography. Microfractographic examinations of tensile fracture surfaces were carried out using scanning electron microscope.

### 3. RESULTS AND DISCUSSION

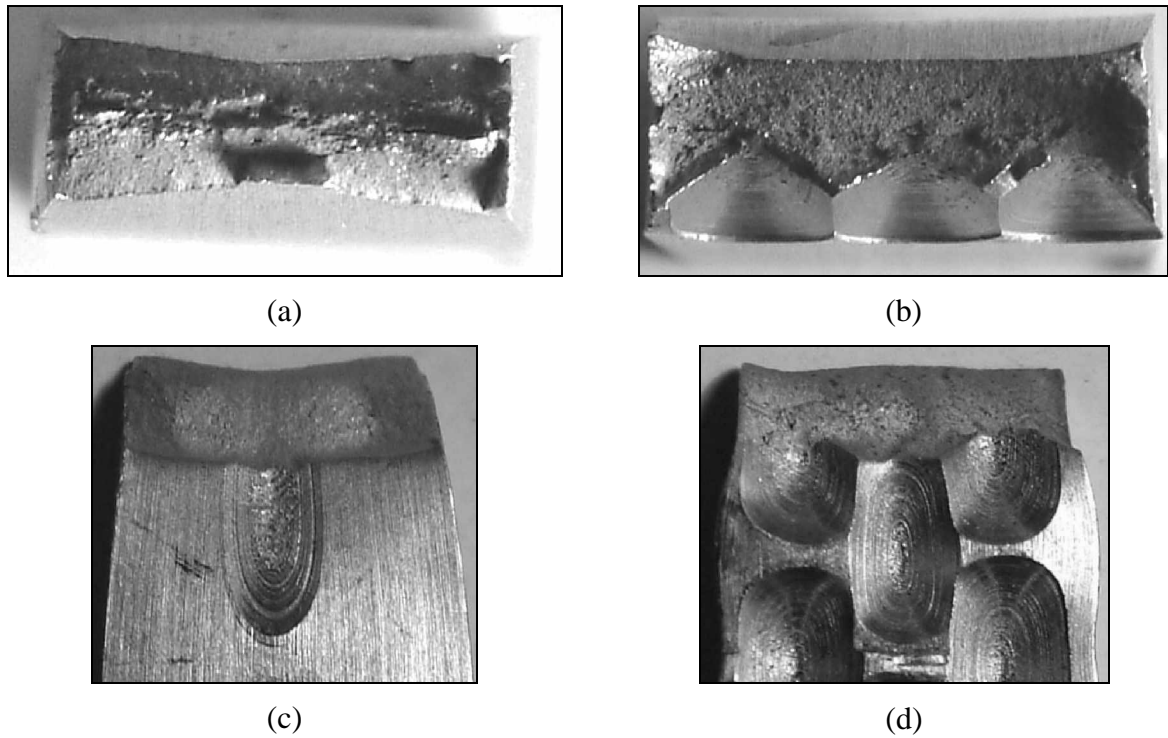
#### 3.1 Fractography

Figure 4(a,b) shows a tensile specimen with a single pit (A2) before and after the test. It can be seen that the fracture plane passes through the reduced cross section at the center of the pit. Similar behavior was observed in other specimens with various pit distributions as shown in Figure 4(c,d).



**Figure 4.** Tensile test specimens (a) with a single pit, and fracture planes of specimens with (b) a single pit, (c) three pits and (d) 12 pits.

The Macroscopic fracture surface of the specimen with no pits is shown in Figure 5(a). The fracture surface exhibits shear lips with a small rough flat region at the center. The effect of pit distribution on macroscopic fracture behavior can be evaluated based on the fracture surface appearance and fracture surface orientation of specimens with various pit distributions shown in Figure 5(b-d). It can be seen from Figure 5(b) that presence of three pits in a single row is capable of changing the fracture surface orientation to a flat surface with small shear lips at specimen corners. Whereas, the other pit distributions shown in Figure 5(c,d) have induced a change to a completely slant fracture surface orientation.



**Figure 5.** Macroscopic appearance and orientation of fracture surfaces in specimens containing (a) no pits, (b) three pits, (c) a single pit and (d) 32 pits.

SEM fractographs showing the fracture surface morphology near the pits are shown in Figure 6(a-d). Extensive secondary cracking near the pits in Figure 6(a,c) is indicative of the intense triaxial stresses acting in these regions during the fracture process. It can be seen from Figure 6(b,d) that the dimpled fracture morphology is dominant on the main fracture surface as well as along the fracture path of secondary cracks. Extensive secondary cracking near the pits in Figure 6(a,c) is indicative of the intense triaxial stresses acting in these regions during the fracture process.

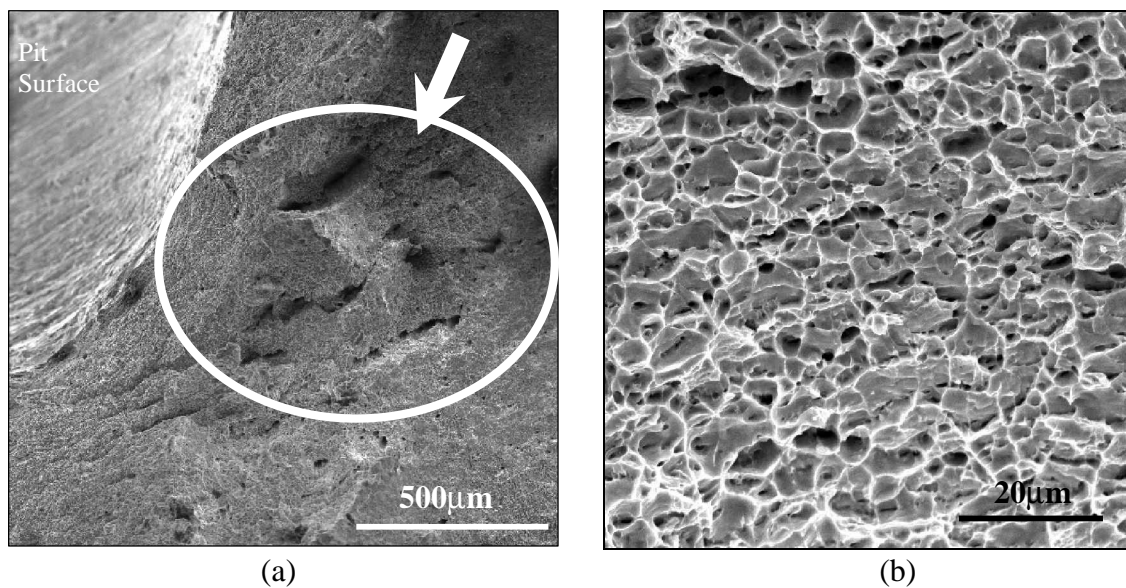


**Figure 6.** Continued in the next page.

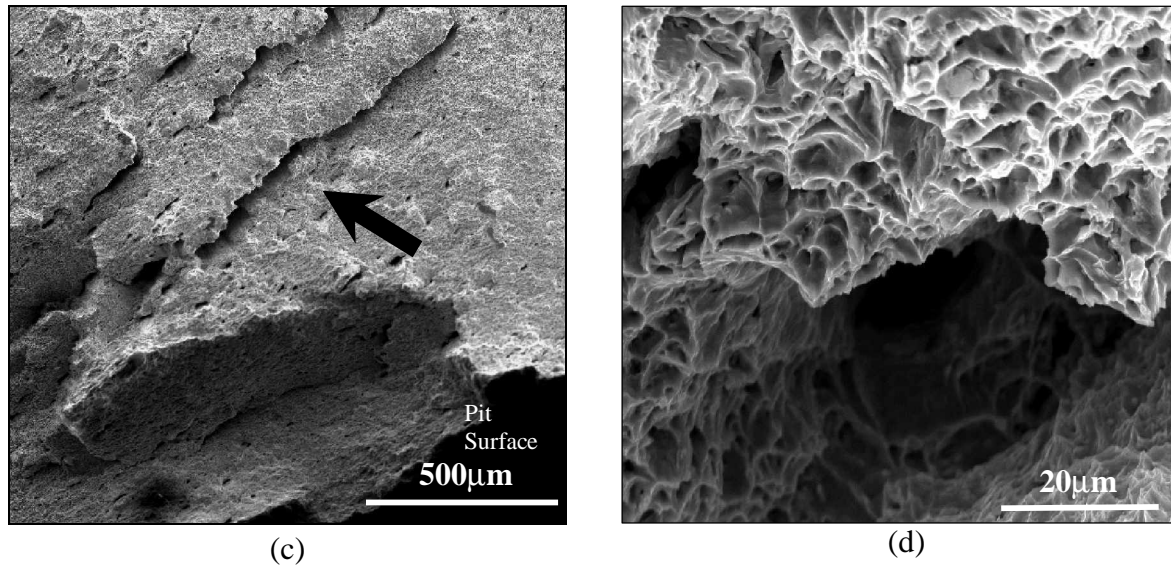


**Figure 6.** SEM fractographs showing (a) secondary cracking in the vicinity of a pit, (b) general dimpled morphology of the fracture surface, (c) Extensive secondary cracking near a pit and (d) secondary cracking by void coalescence.

It can therefore be said that depending on the severity of stress concentration effect and the triaxial stress distribution patterns that is developed by pit distributions various types of fracture surface orientations including slant and flat fracture could be promoted. Furthermore presence of pits also encourages extensive secondary cracking in localized regions ahead of the pits. The macroscopic and microscopic changes in fracture behavior induced by various pit distributions are expected to have a pronounced influence on tensile strength and ductility properties. Effects of primary variables associated with pit distributions including pith depth, pit spacing and pit area percent (PAP) on tensile properties are presented and discussed in the following sections.

### 3.2 Effects of pit distribution variables on tensile properties

#### 3.2.1 Pit depth

Tensile strength as a function of PAP for different artificial pit depths of 0.5, 1 and 1.5 mm, is plotted in Figure 7(a). A generally small reduction of tensile strength can be observed with increasing PAP at a pit depth of 0.5 mm. However, the reduction in tensile strength is substantially intensified at higher pit depths. This trend can be attributed to the higher stress concentration factor and the lower net cross section area associated with deeper piths. Furthermore, all the above curves exhibit an initially sharp drop in tensile strength leading to a minimum point at a PAP of 8%. This indicates that the introduction of first few pits exerts a strong influence on tensile strength. At higher values of PAP, especially at pith depths of 0.5 and 1 mm, the tensile strength remains relatively constant mainly due to the same net cross section area at the fracture location in the various pit distributions investigated.

A similar but more intense trend of initial reduction in final elongation with PAP can be observed in Figure 7(b). However, this sharp reduction of final elongation seems to be partially recovered with increasing PAP, especially at the higher pith depth of 1.5 mm. The initial sharp drop can be attributed to the intense triaxial stress state and strain localization in the vicinity of the pits. These effects are observed to be partly relaxed at higher PAP values, which is primarily due to the mutual interaction of multiple stress concentration sites [5].

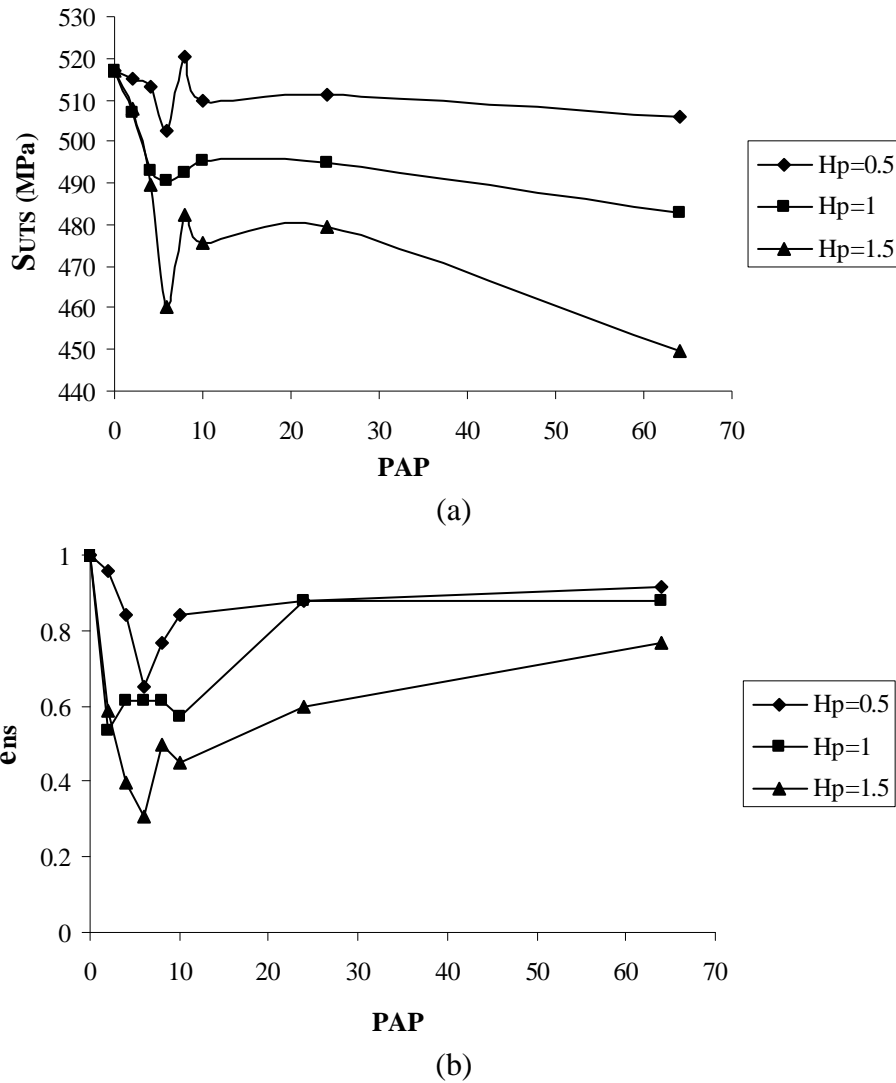
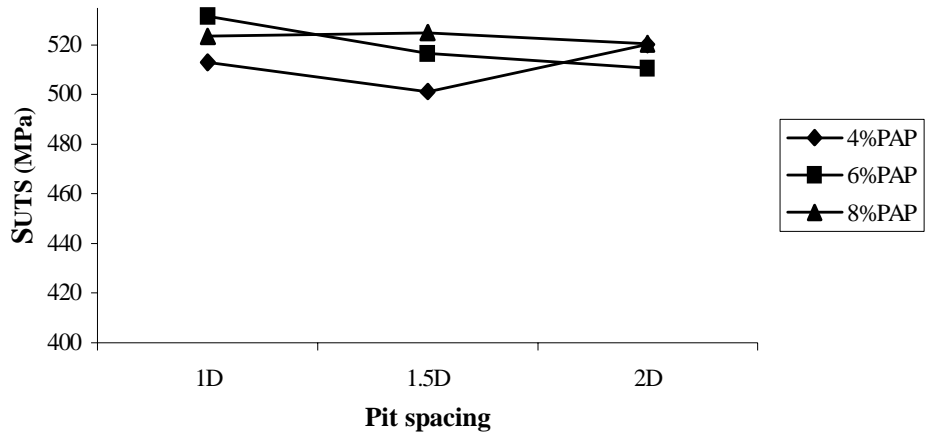


**Figure7.** Tensile strength and final elongation as a function of PAP at different pit depths.

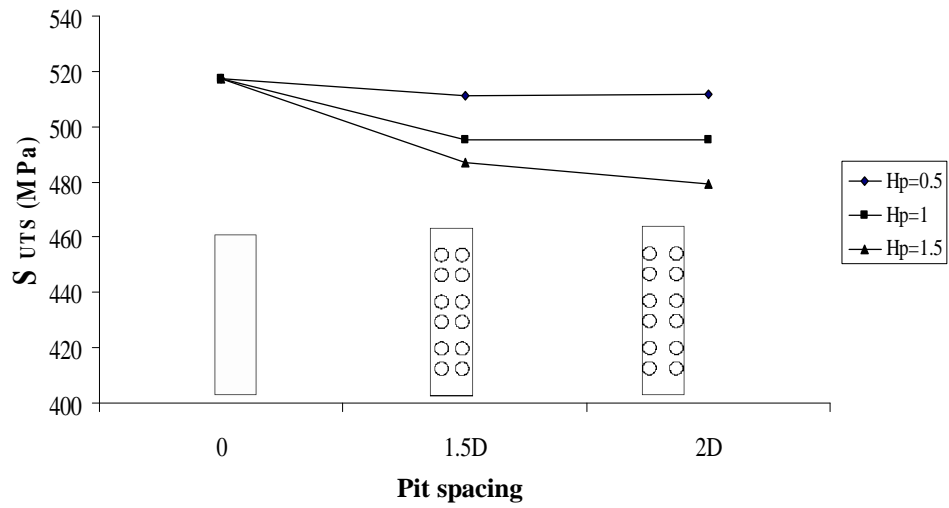
### 3.2.2 Pit spacing

Tensile strength against pit spacing is plotted in Figure 8(a,b). As shown in Figure 8(a), at low PAP values no substantial change in tensile strength with pit spacing is seen for specimens containing 0.5 mm deep pits. However, at higher PAP of 24% a more noticeable drop in tensile strength is observed with increasing pit spacing, especially for specimens containing the deepest pits (1.5 mm), as shown in Figure 8(b). In other words, the stress concentration associated with deeper and denser pit distributions can not be properly relaxed even with increasing pit spacing, in the range studied. Previous studies on tensile specimens containing two similar holes, has shown that the interaction between the two adjacent stress concentration sites, diminishes for  $L > 3D$  [9].

Figure 9(a,b) show the relationship between percent final elongation and pit spacing. Figure 9(a) shows that the initial drop in percent final elongation, following introduction of two closely spaced pits, is partly recovered with increasing pit spacing for specimens with PAP of 4% having two pits of 0.5 mm depth. A similar trend can be observed for specimens with a PAP of 6% and various pit depths in Figure 9(b). It can be argued that denser and more closely spaced pit distributions lead to a more substantial decrease in tensile properties due to the increased stress concentration and strain localization.

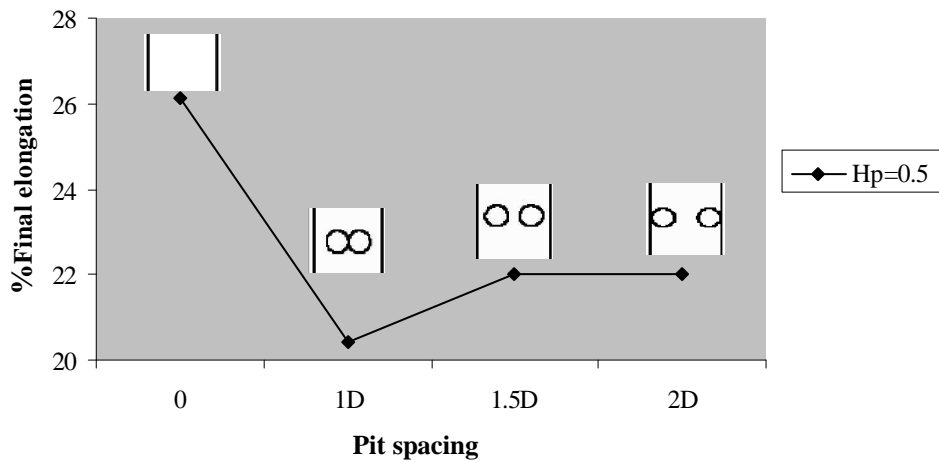


(a)



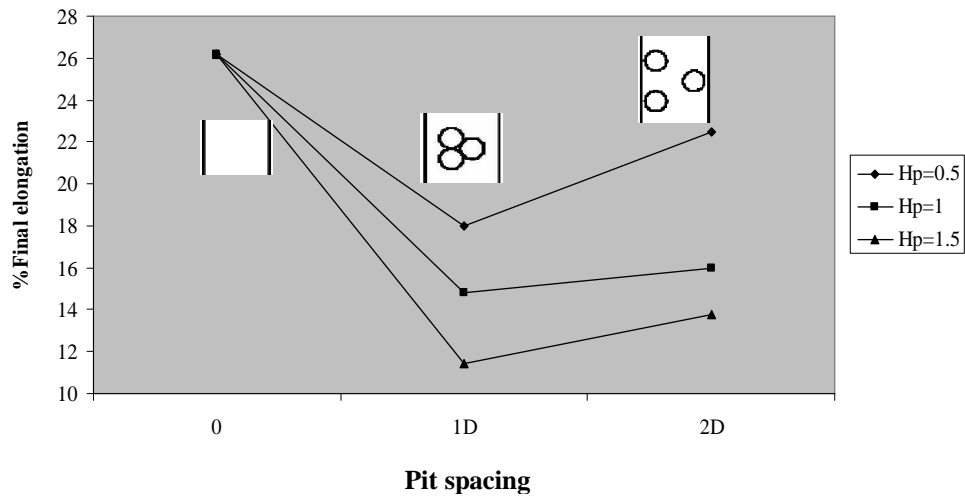
(b)

**Figure 8.** Tensile strength against pit spacing (a) at 0.5 mm pit depth and (b) PAP of 24%.



(a)

**Figure 9.** Continued in the next page.



(b)

**Figure 9.** Percent final elongation versus pit spacing at (a) PAP value of 4% and (b) 6%.

### 3.3 Notch strengthening

In present research CNS, notch strengthening coefficient, is defined by the following equation:

$$C_{NS} = S'_{uts}(N) / S_{uts}$$

Where  $S_{uts}$  is the ultimate tensile strength of specimen without any pits and  $S'_{uts}(N)$  is the net tensile strength of pitted specimens. In the present study, the net ultimate strength is defined by the following equation:

$$S'_{uts}(N) = F_{max} / A$$

$F_{max}$  and  $A$  are the maximum load and the cross section area at the fracture plane (not original cross-sectional area), respectively. Also notch elongation coefficient,  $e_{NS}$ , is defined as final elongation of pitted specimens divided by final elongation of specimen without pit. The changes of  $e_{NS}$  and  $C_{NS}$  with area percent of pit is presented in Figure 10.

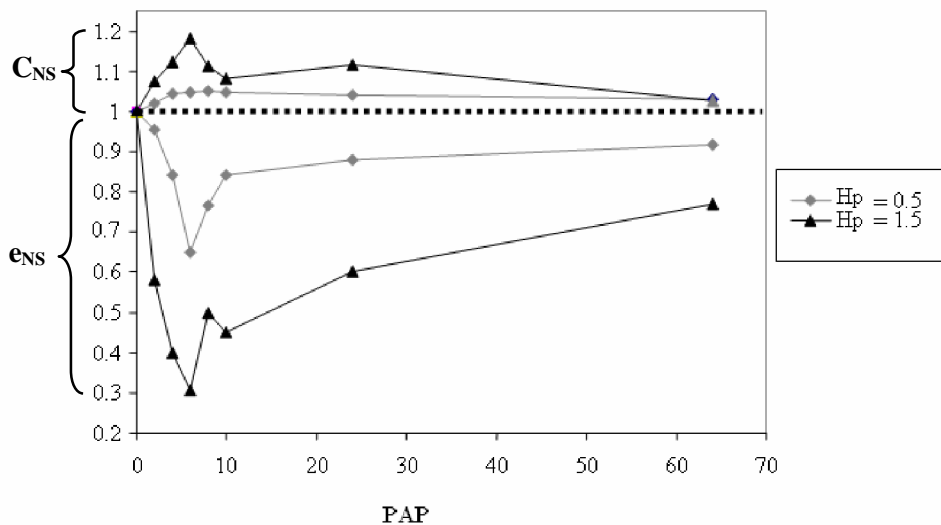


**Figure 10.** The changes in  $e_{NS}$  and  $C_{NS}$  as a function of PAP.

It is seen that  $C_{NS}$  increases with increasing PAP. It is clear that the triaxial stress state set up in pitted specimen leads to a limited increase in net tensile strength of up to 20%. But at the same time the notch elongation coefficient decreases drastically by up to 70%. This significant reduction of final elongation and ductility could promote brittle fracture behavior in pitted structural materials, especially under the influence of aggressive environments. It is clear that the introductions of first few pits and their growth to larger depths could be very detrimental to the mechanical properties of structural alloys.

#### 4. CONCLUSIONS

- 1- Depending on the severity of stress concentration effect and the triaxial stress state pattern that is developed by any given pit distribution various types of fracture surface orientations including slant and flat fracture modes could be promoted.
- 2- Presence of pits leads to extensive secondary cracking in localized regions ahead of the pits during the fracture process.
- 3- Increasing PAP (Pit Area Percent) leads to a general drop in tensile strength which is more intense at lower PAP values of up to 8%. This is attributed to higher stress concentration and smaller net cross section area associated with increasingly denser pit distributions.
- 4- A more significant reduction in final elongation is observed with increasing PAP which tends to be largely recovered at higher PAP values due to increasing uniformity of strain distribution.
- 5- More closely spaced pit distributions lead to a more substantial decrease in tensile properties due to the increased stress concentration and strain localization especially encountered at higher pit depths.
- 6- The final elongation is strongly influenced by the pit depth at low PAP values, such that a maximum of 70% reduction in final elongation is observed at the highest pit depth of 1.5 mm studied.

#### ACKNOWLEDGEMENTS

The authors acknowledge the helpful assistance of Eng. F. Hassanabadi during the study.

#### REFERENCES

1. Dieter, G., **Mechanical Metallurgy**, 3rd edition, Mc Graw Hill, 2001.
2. Hertzberg, R.W., **Deformation and Fracture Mechanics of Engineering Materials**, John Wiley & Sons, 3<sup>rd</sup> ed., Canada, 1989.
3. ASM, **Metals Handbook: Corrosion**, Vol. 13, 10<sup>th</sup> ed., Materials Park, OH, 1990.
4. Paik, J.K., Lee, J.M., Park, Y.I., Hwang, J.S., Kim, C.W., "Time-variant ultimate longitudinal strength of corroded bulk carriers", *Marine structures* 16, 2003, pp. 567-600.
5. Nakai, T., Matsushita, H., Yamamoto, N., Arai, H., "Effect of pitting corrosion on local strength of hold frames of bulk carriers (1<sup>st</sup> report)", *Marine structures*, 17, pp. 403-432, 2004.
6. Naki, T., Matsushita, H., Yamamoto, N., Arai, H., "Effect of pitting corrosion on local strength of hold frames of bulk carriers (2<sup>nd</sup> report) – Lateral-Distortional buckling and local face buckling", *Marine structures* 17, pp. 612-64, 2004.
7. Gardiner, C.P., Melchers, R.E., "Corrosion of mild steel by coal and iron ore", *Corrosion Science* 44, pp. 2665-2673, 2002.
8. Nakai, T., Matsushita, H., Yamamoto, N., Arai, H., "Pitting corrosion and its influence on local strength of hull structural members", 24<sup>th</sup> International conference on offshore mechanics and arctic engineering, Greece, pp.1-11, 2005.
9. Pilkey, W.D., **Peterson's Stress Concentration Factors**, John Wiley & Sons, 2<sup>nd</sup> ed., Canada, 1997.